Physica **96A** (1979) 487–505 © *North-Holland Publishing Co.*

BLOCK DIAGRAMS AND THE CANCELLATION OF DIVERGENCIES IN ENERGY-LEVEL PERTURBATION THEORY

M.A.J. MICHELS‡ and L.G. SUTTORP

Instituut voor theoretische fysica, Universiteit van Amsterdam, Valckenierstraat 65, 1018 XE Amsterdam, The Netherlands

Received 26 January 1979

The effective Hamiltonian for the degenerate energy-eigenvalue problem in adiabatic perturbation theory is cast in a form that permits an expansion in Feynman diagrams. By means of a block representation a resummation of these diagrams is carried out such that in the adiabatic limit no divergencies are encountered. The resummed form of the effective Hamiltonian is used to establish a connexion with the S matrix.

1. Introduction

Perturbation theory for degenerate energy levels can be formulated with the help of an effective Hamiltonian. In the adiabatic approach this Hamiltonian is expressed in terms of chronological products of interaction operators, so that Wick's theorem may be applied. As a consequence, the energy shifts of a perturbed degenerate level are found through the evaluation of a set of Feynman diagrams. This method has been used frequently in calculations of nuclear structure and molecular interactions[1]). In particular, lowest-order perturbation theory leads to a simple form for the effective Hamiltonian, which may be understood heuristically on the basis of the Born approximation[2]). When higher-order perturbation theory is employed the diagrammatic representation of the effective Hamiltonian becomes more complicated. For the special case of instantaneous interactions the introduction of so-called 'folded' diagrams has proved advantageous[3–5]). The field-theoretical perturbation theory for non-instantaneous interaction has so far been studied only in specific problems, as for instance molecular energy and polarizability calculations in quantum electrodynamics[6–12]). In these examples it was found that some of the occurring Feynman diagrams are divergent in the adiabatic limit; to calculate the energy shifts a resummation of the divergent diagrams had to be performed. The purpose of the present paper is to show how the diagrammatic expansion of the effective Hamiltonian for general interactions can generally be resummed so as to yield a termwise finite

‡ Present address: Koninklÿke/Shell-Laboratorium, Amsterdam.

result in the adiabatic limit. The analysis is facilitated by a schematic block representation of the Feynman diagrams, which clearly displays the origins of the divergencies.

The paper has been organized as follows. In section 2 the field-theoretical expression for the full effective Hamiltonian, and in particular for the averaged energy shift, is derived from adiabatic perturbation theory. In the next section the cancellation of divergencies is demonstrated for the example of interatomic two-photon exchange processes. A reformulation of this cancellation is given in section 4, where the concept of block diagrams is introduced. In section 5 more general examples of the resummation of diagrams are worked out, while in section 6 the general rules are established for obtaining termwise finite diagram expansions for the averaged energy shift. In section 7 it is shown how these rules are to be extended when the full effective Hamiltonian is considered. After the resummation procedure has been carried out the averaged energy shift can be related to the S matrix, as will be proved in the last section.

2. The effective Hamiltonian in the adiabatic formalism

We shall study a stationary system with an unperturbed Hamiltonian H_0. Let P_0 be the projector on a degenerate level in the discrete part of the spectrum of H_0. When a time-independent perturbation H_1 is present the energy shifts ΔE of such a level may be found as the eigenvalues of an effective Hamiltonian $V = P_0 V P_0$. The relation between V and the interaction H_1 can be established either by time-independent methods[13,14]) or with the help of the adiabatic formalism[3-5,15-19]). In the latter case the time-dependent interaction picture is used; in addition an explicit time dependence is introduced by adiabatically switching on the interaction. The total Hamiltonian then gets the form:

$$H_0 + \mathrm{e}^{-\epsilon|t|} H_1(t) = H_0 + \mathrm{e}^{-\epsilon|t|}\, \mathrm{e}^{\mathrm{i}H_0 t} H_1\, \mathrm{e}^{-\mathrm{i}H_0 t}, \tag{1}$$

while the time evolution of the system is governed by the evolution operator:

$$U_\epsilon(t, t') = \sum_{n=0}^{\infty} (-\mathrm{i})^n \int_{t'}^{t} \mathrm{d}t_1 \ldots \mathrm{d}t_n\, \mathrm{e}^{-\epsilon|t_1| \cdots - \epsilon|t_n|} H_1(t_1)\theta(t_{12}) \times H_1(t_2)\theta(t_{23}) \ldots H_1(t_n), \tag{2}$$

with $t_{ij} = t_i - t_j$. In terms of U_ϵ one finds for the effective Hamiltonian:

$$V = \lim_{\epsilon \to 0} P_0 H_1 U_\epsilon(0, -\infty) P_0 [P_0 U_\epsilon(0, -\infty) P_0]^{-1}. \tag{3}$$

The operator $P_0U_\epsilon(0,-\infty)P_0$ is the sum of the zeroth-order projector P_0 and a term $P_0\{U_\epsilon(0,-\infty)-1\}P_0$, which vanishes in the absence of a perturbation. Hence the power series of the function $(1+x)^{-1}$ can be applied in (3) to the inverse $[P_0U_\epsilon(0,-\infty)P_0]^{-1}$. When moreover (2) is substituted we obtain for V the perturbation expansion[19]):

$$V=\lim_{\epsilon\to 0}\sum_{n=1}^{\infty}(-\mathrm{i})^{n-1}\int_{-\infty}^{0}\mathrm{d}t_1\ldots\mathrm{d}t_{n-1}\,\mathrm{e}^{-\epsilon|t_1|-\ldots-\epsilon|t_{n-1}|}$$
$$\times P_0H_1(0)\{\theta(-t_1)-P_0\}H_1(t_1)\{\theta(t_{12})-P_0\}\ldots H_1(t_{n-1})P_0. \tag{4}$$

At the right-hand side we shall split up the contribution of a given order n into terms with N time-ordered products of interaction operators, the jth product having k_j factors $H_1(t)$; upon symmetrizing the products with respect to the time variables and introducing the time-ordering symbol T the expression (4) becomes:

$$V=\lim_{\epsilon\to 0}\sum_{n=1}^{\infty}(-\mathrm{i})^{n-1}\int_{-\infty}^{\infty}\mathrm{d}t_1\ldots\mathrm{d}t_n\,\mathrm{e}^{-\epsilon|t_1|-\ldots-\epsilon|t_n|}\delta(t_{\max})$$
$$\times\sum_{N=1}^{\infty}\sum_{k_1,\ldots,k_N=1}^{\infty\,\prime}\sum_{i=1}^{k_1}\prod_{j(\neq i)}^{n}\theta(t_{ij})\frac{(-1)^{N-1}}{k_1!\ldots k_N!}$$
$$\times P_0T[H_1(t_1)\ldots H_1(t_{k_1})]P_0T[H_1(t_{k_1+1})\ldots H_1(t_{k_1+k_2})]\ldots$$
$$P_0T[H_1(t_{n-k_N+1})\ldots H_1(t_n)]P_0. \tag{5}$$

Here the prime at the summation sign stands for the restriction $\Sigma_{j=1}^{N}k_j=n$. The condition on the upper boundaries of the time integrations is expressed formally through a product of δ and θ functions. In fact it merely states that the maximum $t_{\max}$ of $t_1,\ldots,t_n$ is equal to zero, and that this maximum is to be chosen symmetrically out of the time variables $t_1,\ldots,t_{k_1}$ of the leading time-ordered product.

If one is not interested in the full effective Hamiltonian V but only in the average energy shift $\overline{\Delta E}$ of the degenerate level, the discussion may be limited to the trace $\mathrm{Tr}\,V=\overline{\Delta E}\,\mathrm{Tr}\,P_0$. In that case the integrand of (5) may be made cycle-symmetric by choosing $t_{\max}$ in any of the time-ordered products. Then the trace of the effective Hamiltonian can be written as:

$$\mathrm{Tr}\,V=\lim_{\epsilon\to 0}\sum_{n=1}^{\infty}(-\mathrm{i})^{n-1}\int_{-\infty}^{\infty}\mathrm{d}t_1\ldots\mathrm{d}t_n\,\mathrm{e}^{-\epsilon|t_1|-\ldots-\epsilon|t_n|}$$
$$\times\delta(t_{\max})\sum_{N=1}^{\infty}\sum_{k_1,\ldots,k_N=1}^{\infty\,\prime}\frac{(-1)^{N-1}}{Nk_1!\ldots k_N!}$$
$$\times\mathrm{Tr}\{P_0T[H_1(t_1)\ldots H_1(t_{k_1})]P_0T[H_1(t_{k_1+1})\ldots H_1(t_{k_1+k_2})]\ldots$$
$$P_0T[H_1(t_{n-k_N+1})\ldots H_1(t_n)]\}. \tag{6}$$

The equations (5) and (6) show that in the interaction representation the energy-eigenvalue problem of a perturbed degenerate level may be formulated entirely in terms of symmetric time-ordered products of the perturbation. If the Hamiltonian H_0 of the unperturbed system and the perturbation H_1 can be described by quantum field theory the ensuing time-ordered products of field operators may be dealt with by applying Wick's theorem. In this way the effective Hamiltonian is represented by a set of Feynman diagrams. However, evaluation of the individual diagrams by standard field-theoretical methods will generally not be possible, since the existence of the adiabatic limits is guaranteed only for the complete set of diagrams contributing to a particular order n in (5) and (6). To avoid divergencies a resummation of the Feynman diagrams is necessary; in the following sections it will be shown how this resummation is achieved in terms of generalized Feynman diagrams that can indeed be calculated separately in the adiabatic limit.

3. Resummation of diagrams in fourth order

As an example of the field-theoretical perturbation theory we shall consider the two-photon exchange contribution to the interaction of two hydrogen atoms a, b in their ground states[6,7,9-11]). In accordance with the Born–Oppenheimer approximation the nuclei are held fixed, while the electrons are described by the covariant Dirac theory. For convenience we shall confine ourselves to the electronic part of the photon-exchange interaction, which follows from the Hamiltonian $H_1 = -e \int \mathrm{d}x \bar{\psi} \gamma_\mu \psi A^\mu$, with ψ and A^μ the electron and photon fields; the nuclear part can be treated in an analogous way.

The interaction energy will be averaged over the twofold degenerate ground states α_0, β_0 of both atoms independently, so that the formula (6) can be used. In the summations over N and k_j only two terms contribute to this fourth-order process, *viz* with $N = 1$, $k_1 = 4$ and with $N = 2$, $k_1 = k_2 = 2$. Carrying out all possible contractions one gets the set of Feynman diagrams of fig. 1. The first diagram yields for Tr V:

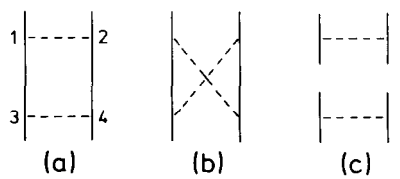

Fig. 1. Feynman diagrams for interatomic two-photon exchange, (a, b) with $N = 1$, and (c) with $N = 2$.

$$\lim_{\epsilon\to 0}\sum_{\alpha_0,\beta_0} ie^4\int d^4x_1\ldots d^4x_4\, e^{-\epsilon|t_1|\ldots-\epsilon|t_4|}\delta(t_{\max})$$
$$\times\bar\psi_{\alpha_0}(x_1)\gamma^\kappa S_{Fa}(x_1,x_3)\gamma^\mu\psi_{\alpha_0}(x_3)\bar\psi_{\beta_0}(x_2)\gamma^\lambda S_{Fb}(x_2,x_4)$$
$$\times\gamma^\nu\psi_{\beta_0}(x_4)g_{\kappa\lambda}g_{\mu\nu}D_F(x_{12})D_F(x_{34}). \tag{7}$$

Here the photon propagator reads:

$$iD_F(x) = -\theta(t)\frac{1}{(2\pi)^3}\int\frac{dk}{2k}e^{ik\cdot x-ik^0t} - \theta(-t)\frac{1}{(2\pi)^3}\int\frac{dk}{2k}e^{ik\cdot x+ik^0t}$$
$$= -\frac{i}{(2\pi)^3}\int d^4k\,\frac{e^{ik\cdot x-ik^0t}}{k^{02}-k^2+i0}; \tag{8}$$

the electron propagator is a sum over positive- and negative-energy bound-state solutions:

$$iS_F(x,x') = \theta(t-t')\sum_{E>0}\psi(x)\bar\psi(x')\,e^{-iE(t-t')} - \theta(t'-t)\sum_{E<0}\psi(x)\bar\psi(x')\,e^{-iE(t-t')}. \tag{9}$$

When (9) is substituted the expression (7) becomes a summation over positive- and negative-energy intermediate states for both atoms. The part with ground-level intermediate states reads:

$$\lim_{\epsilon\to 0}\sum_{\alpha_0,\beta_0,\alpha_0',\beta_0'} -ie^4\int d^4x_1\ldots d^4x_4\, e^{-\epsilon|t_1|\ldots-\epsilon|t_4|}$$
$$\times\delta(t_{\max})F(t_1,\ldots,t_4)\bar\psi_{\alpha_0}(x_1)\gamma^\kappa\psi_{\alpha_0'}(x_1)\bar\psi_{\alpha_0'}(x_3)\gamma^\mu\psi_{\alpha_0}(x_3)$$
$$\times\bar\psi_{\beta_0}(x_2)\gamma^\lambda\psi_{\beta_0'}(x_2)\bar\psi_{\beta_0'}(x_4)\gamma^\nu\psi_{\beta_0}(x_4)g_{\kappa\lambda}g_{\mu\nu}D_F(x_{12})D_F(x_{34}), \tag{10}$$

with $F=\theta(t_{13})\theta(t_{24})$. This contribution to Tr V is divergent in the adiabatic limit, as can be seen by actually performing the time integrations. In fact, the divergence can be read off already from the diagram 1a, since the order of the vertices can be chosen such that at a fixed intermediate time the total energy of the system equals that of the initial state; this argument will be made more specific in the appendix. A similar situation does not occur in the diagram 1b, owing to the different contraction of the photon lines. The contribution of the product diagram 1c has the same form as (10), with $F=-\frac{1}{2}$, and is likewise divergent when ϵ is put equal to zero.

In view of the existence of the adiabatic limit for the total effective Hamiltonian V the divergencies in figs. 1a and 1c should cancel. To make this cancellation explicit we first symmetrize the integrand in (10) with respect to the vertex pairs (1, 2) and (3, 4). The sum of the terms with ground-level intermediate states in Tr V then contains a time-ordering factor F of the form:

$$\tfrac{1}{2}[\theta(t_{13})\theta(t_{24})+\theta(t_{31})\theta(t_{42})-1] = -\tfrac{1}{2}[\theta(t_{13})\theta(t_{42})+\theta(t_{31})\theta(t_{24})]. \tag{11}$$

In both terms at the right-hand side time orderings with $t_1 > t_3$, $t_2 > t_4$ or $t_3 > t_1$, $t_4 > t_2$ are excluded, so that indeed at no fixed intermediate time the system has an energy equal to that of the initial state; hence the resulting time integral remains finite in the adiabatic limit, so that the averaged interaction energy of the atoms can now be found straightforwardly. The detailed calculations have been given elsewhere[9,11]).

4. Block-diagram representation of the averaged energy shift

In the preceding section it was shown for the special case of interatomic photon-exchange interactions how the contributions of the various Feynman diagrams could be rearranged in such a way that all terms are separately convergent in the adiabatic limit. In order to generalize this treatment it is useful to introduce a more schematic representation for Feynman diagrams connecting identical initial and final energy levels. For convenience we shall limit ourselves to initial states $|\psi_0\rangle$ that are products $\Pi_k|\psi_{k0}\rangle$ of positive-energy states $|\psi_{k0}\rangle$ of distinguishable particles $k = a, b, \ldots$. The interactions are supposed to conserve particle number of each species k separately.

Let us split the Feynman propagators $S_{F,k}$ $(k = a, b, \ldots)$ that occur in a diagram D into two parts $S^0_{F,k}$ and $S'_{F,k}$; the contribution $S'_{F,k}$ contains a sum over the k-states with energies different from that of the initial state $|\psi_{k0}\rangle$, whereas $S^0_{F,k} = S_{F,k} - S'_{F,k}$ involves only the initial-level states. In the example of section 3, the part S^0_F of the electron propagator (9) becomes in this way:

$$iS^0_F(x, x') = \theta(t - t') \sum_{E=E_0} \psi(x)\bar{\psi}(x')\, e^{-iE_0(t-t')}, \tag{12}$$

with E_0 the ground-level energy.

When the above splitting is carried out for all internal lines of the types $k = a, b, \ldots$, the diagram D becomes a sum of diagrams D_L in which the internal k-lines carry an additional label 0 or '. The vertices in such a labelled diagram may be grouped now in blocks that are defined as the smallest units into which D_L falls apart if all propagator lines $S^0_{F,k}$ are cut. In this way one arrives at a schematic block representation D_B of a labelled diagram D_L; a general Feynman diagram D can then be written as a sum of these block diagrams.

A pair of blocks in a diagram D_B may be either disconnected (as is the case for product diagrams like fig. 1c or connected by one or more parallel $S^0_{F,k}$ lines. Each of these lines carries a time factor $\theta(t_{kI} - t_{kII})$ or $\theta(t_{kII} - t_{kI})$ with k_I and k_{II} vertices in the blocks I and II, respectively. For the product $\Pi_k\theta(t_{kI} - t_{kII})$ of all θ functions directed from II to I we shall introduce as a short-hand

notation the symbol $\Theta_{I,II}$. Correspondingly, in the diagram the associated propagator lines will be contracted into one oriented line →—. In general, a factor $\Theta_{II,I}$ will occur as well so that the blocks I and II will be linked by two lines with opposite orientations.

The above procedure to introduce block diagrams may be illustrated with the help of the diagrams of fig. 1. The Feynman diagram 1a is a sum of four labelled diagrams. The contribution with 0-labels at both intermediate electron lines consists of two identical blocks I and II, with vertices 1, 2 and 3, 4, respectively (see fig. 2a); the intermediate time factor reads $\Theta_{I,II} = \theta(t_1 - t_3)\theta(t_2 - t_4)$. The other three contributions from fig. 1a, with a prime at one or both electron lines, may each be represented by the single block of fig. 2b; the diagram of fig. 1b remains one block for all labellings of electron lines, owing to the occurrence of crossed photon lines. Finally the product diagram 1c is built up of two separate blocks as drawn in fig. 2c.

In section 3 we have shown how the divergent contributions that are represented by the block diagrams 2a and 2c may be grouped such that a finite result is found. This resummation applies quite generally to two-block diagrams of the type of fig. 2. In fact, the time factor from the diagrams 2a and 2c is $\Theta_{I,II} - \frac{1}{2}$ (*v.* section 3). In view of the symmetry between the blocks I and II we may replace the diagram 2a by half the sum of 2a and 2d. The total time factor then becomes:

$$\tfrac{1}{2}(\Theta_{I,II} + \Theta_{II,I} - 1) = \tfrac{1}{2}[\Theta_{I,II}\Theta_{II,I} - (\Theta_{I,II} - 1)(\Theta_{II,I} - 1)]. \tag{13}$$

It should be noted that $\Theta_{ij} - 1$ will in general be different from $-\Theta_{ji}$. For the particular case of section 3 the product $\Theta_{I,II}\Theta_{II,I}$ gives a vanishing contribution, since it there implies incompatible requirements on the time variables. In general however, this product does contribute, as is clear for instance when each block is thought to contain a two-photon exchange process with crossed photon lines.

After the resummation in (13) the two terms at the right-hand side may be considered in their turn as the time factors of new block diagrams. According to the rules given already the first term will correspond to the diagram 3a; the main difference with the diagrams of fig. 2 consists in the occurrence of a

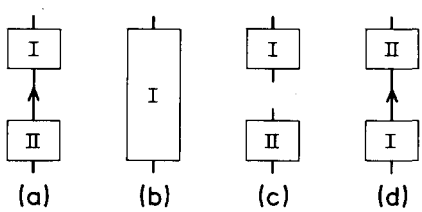

Fig. 2. Block diagrams for the two-photon exchange process of fig. 1.

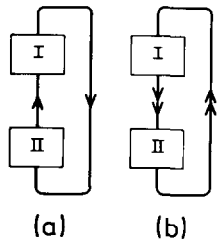

Fig. 3. Finite block diagrams resulting from the resummation of fig. 2.

closed loop of two oriented lines between the blocks. The second term in (13) may be represented in a similar way. To that end we make the convention to denote a factor $\Theta_{ij} - 1$ by an oriented line $\rightarrow\!\!\!\!\!\!\rightarrow$ pointing from block i to j; then one arrives at the diagram of fig. 3b, which again contains a closed loop.

The block diagrams introduced here have the convenient property that one may assess the finiteness of the corresponding terms in the energy shift without a detailed knowledge of the internal structure of the blocks. To exemplify this we shall prove now that the block diagrams of fig. 3 each yield a finite contribution. As has been argued already in connexion with eq. (11) of section 3, the time integrations for a particular diagram may yield an infinite result only if an ordering of the vertices can be chosen that allows an intermediate state at time t with energy equal to that of the initial state. The existence of such an intermediate state implies that at constant time t an intersection of the diagram can be made through a number of 0-lines only. By definition a block cannot be split into two parts by an intersection of 0-lines. Furthermore, the explicit factors Θ and $\Theta - 1$ between the blocks, represented by the lines with single and double arrows, forbid a relative time ordering of the blocks such that all vertices in one block have times t smaller than those of all vertices in the other block. As a consequence the occurrence of intermediate states with initial-state energy is ruled out completely, which proves the finiteness of the diagrams 3a and 3b.

The method used above to rearrange a sum of divergent two-block diagrams will be generalized now to diagrams with more blocks. In the following we shall first study diagrams consisting of a string of blocks. Subsequently an example of a diagram with a more complicated structure will be considered. In this way we will be led to a general prescription for the rearrangements of block diagrams in such a way that a termwise finite representation of the averaged energy shift is obtained.

The general expression (6) for the trace of the effective Hamiltonian may be written as a sum of block diagrams in the way indicated above. For a block diagram with M blocks the simplest example is drawn in fig. 4a. It results from

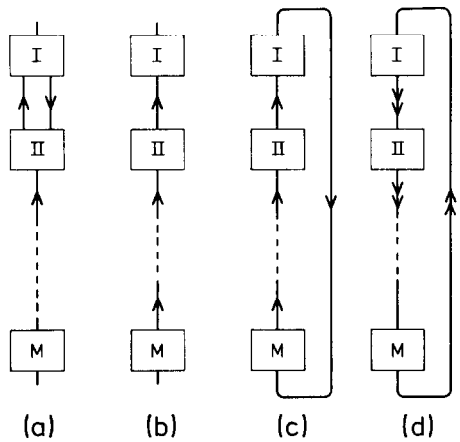

Fig. 4. (a, b) Divergent diagrams for strings of blocks; (c, d) resummed string-type block diagrams.

the term with $N = 1$ in (6) and consists of a string of blocks connected by arrows in either direction (note that particle conservation forbids the occurrence of single lines pointing downwards). This diagram gives rise to an infinite time integral in the adiabatic limit, since an intersection at constant time is possible through the 0-lines below the block II. No such intersection can be made between the blocks I and II, which are connected by two oppositely oriented lines. When investigating the divergencies of a diagram we can therefore limit ourselves to strings of blocks linked in the way of fig. 4b. The time factor associated with the latter diagram is:

$$\Theta_{\mathrm{I,II}}\Theta_{\mathrm{II,III}} \ldots \Theta_{\ldots,\mathrm{M}}. \tag{14}$$

Assuming for the present that all blocks have identical internal structure, we may replace the diagram of fig. 4b by a symmetrized sum of M block diagrams obtained by a cyclic permutation of the blocks.

The other terms in the effective Hamiltonian (6), with $N > 1$, likewise yield block diagrams of the form of fig. 4b, with $(N-1)$ out of the $(M-1)$ lines absent; in view of the structure of (6) their time factors follow from (14) by replacing $(N-1)$ factors Θ by -1. For fixed N and M one obtains in this way $(N/M) \times \binom{M}{N}$ different block diagrams. When again a cyclic permutation of the blocks is performed and the explicit factor N^{-1} in (6) is taken into account one arrives, upon summation over all N, at a total time factor:

$$\frac{1}{M}\left[\Theta_{\mathrm{I,II}}\Theta_{\mathrm{II,III}} \ldots \Theta_{\mathrm{M,I}} - (\Theta_{\mathrm{I,II}} - 1)(\Theta_{\mathrm{II,III}} - 1) \ldots (\Theta_{\mathrm{M,I}} - 1)\right]. \tag{15}$$

This formula is a straightforward generalization of the result (13); just as in

that case a factor Θ_{ij} or $\Theta_{ij} - 1$ is present for each line that connects a pair of blocks. The symmetry factor M^{-1} follows from the assumption of identical structure of the blocks. When all blocks are different the only modification is that no such factor shows up; in the case of partial symmetry the appropriate factor is easily determined.

As before we may represent the two terms in (15) by diagrams with single or double arrows only (see fig. 4c and 4d). The blocks are connected by closed loops of a unique orientation; this feature guarantees the finiteness of each diagram separately.

The block diagrams discussed so far are not the most general that may be encountered. A different type is given in fig. 5a, where a new feature is the occurrence of parallel lines, i.e. lines that pass along one of the blocks. Cyclic permutation of the blocks yields in addition the diagrams of fig. 5b and 5c. The total time factor from figs. 5a–c then becomes:

$$\Theta_{\mathrm{I,II}}\Theta_{\mathrm{II,III}}\Theta_{\mathrm{I,III}} + \Theta_{\mathrm{II,III}}\Theta_{\mathrm{III,I}} + \Theta_{\mathrm{I,II}}\Theta_{\mathrm{III,I}}. \tag{16}$$

The product diagrams accompanying these have been drawn in fig. 6; their total time factor is:

$$-\Theta_{\mathrm{II,III}} - \Theta_{\mathrm{III,I}} - \Theta_{\mathrm{I,II}} + 1. \tag{17}$$

The Θ functions in the sum of (16) and (17) must be regrouped now such that the result gives rise to termwise finite contributions in the energy shift. To that end we need a systematic procedure for generalizing the *ad hoc* manipulations performed so far. The characteristic feature of the final expression (15) for the time factor of the string diagram is that each term is a product of factors Θ_{ij} or $\Theta_{ij} - 1$, one for each line that is realized in any of the underlying block diagrams. The same feature may be introduced in the time factors (16) and (17) by inserting a factor $1 = \Theta_{ij} - (\Theta_{ij} - 1)$ for each line (ij)

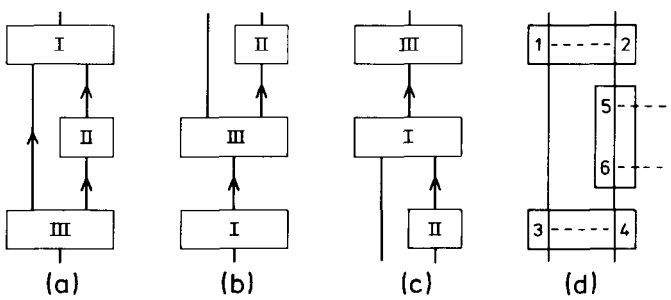

Fig. 5. (a–c) Block diagrams with parallel lines; (d) typical diagram of the atomic pair polarizability, as a physical example of (a).

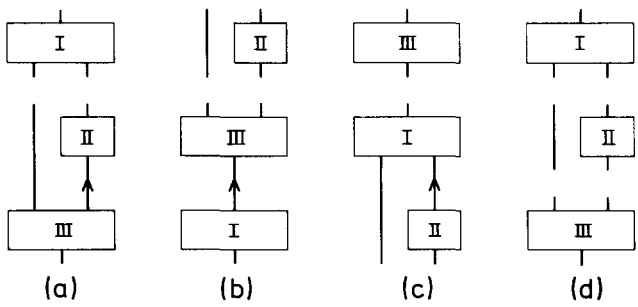

Fig. 6. Intersected block diagrams with parallel lines.

from the set (I, II), (II, III), (I, III), (III, I) that is missing in a particular diagram. In this way the total time factor for the diagrams of figs. 5a–c and 6 is found to be:

$$\Theta_{\mathrm{I,II}}\Theta_{\mathrm{II,III}}\Theta_{\mathrm{I,III}}\Theta_{\mathrm{III,I}} - [\Theta_{\mathrm{I,II}}\Theta_{\mathrm{II,III}}(\Theta_{\mathrm{I,III}}-1) - (\Theta_{\mathrm{I,II}}-1)(\Theta_{\mathrm{II,III}}-1)\Theta_{\mathrm{I,III}} + (\Theta_{\mathrm{I,II}}-1)(\Theta_{\mathrm{II,III}}-1)(\Theta_{\mathrm{I,III}}-1)](\Theta_{\mathrm{III,I}}-1). \tag{18}$$

As before this expression may be represented by diagrams with single and double arrows (see fig. 7). The structure of these diagrams is more complicated than those of fig. 4c, d. In the present case both types of internal lines, with single and double arrows, may occur simultaneously. Nevertheless each of the diagrams in fig. 7 yields a finite contribution to the energy shift, since no time ordering can be found such that all vertices in one or more blocks carry time labels smaller than those of the remaining vertices.

An example of a physical process where block diagrams with parallel lines show up is the dipole polarization of a pair of atoms in an external electric field[12]). A typical diagram that contributes to the energy shift associated with this pair polarization has been drawn in fig. 5d. It gets the block structure of fig. 5a if the appropriate intermediate atomic states are chosen equal to the initial states. When all pair-polarization diagrams of the type of figs. 5a–c and

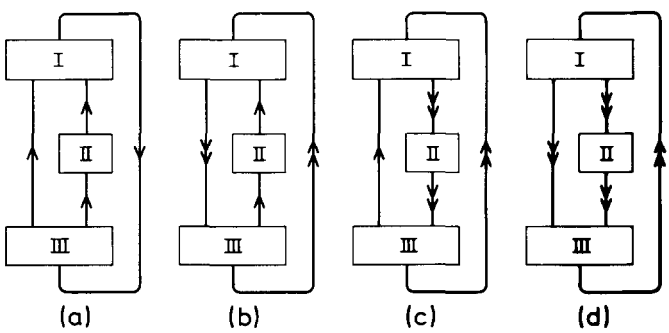

Fig. 7. Resummed block diagrams with parallel lines.

6 are combined one ends up with a total time factor that is in fact a translation of (18):

$$\theta_{25}\theta_{64}\theta_{13}\theta_{31}\theta_{42} - [\theta_{25}\theta_{64}(\theta_{13}-1) - (\theta_{25}-1) \times (\theta_{64}-1)\theta_{13} + (\theta_{25}-1)(\theta_{64}-1)(\theta_{13}-1)](\theta_{31}\theta_{42}-1) = -\theta_{25}\theta_{64}\theta_{31}\theta_{24} - \theta_{52}\theta_{46}\theta_{13}\theta_{24} - \theta_{52}\theta_{46}\theta_{13}\theta_{42} - \theta_{52}\theta_{46}\theta_{31}\theta_{24}. \quad (19)$$

It is checked immediately that neither of these terms gives an infinite result when the time integrals are carried out.

5. General resummation procedure for block diagrams

For the special types of block diagrams treated in the preceding sections we have shown how the diagrams contributing to the energy shift could be rearranged by writing each time factor as a product of functions Θ_{ij} (for each line (ij) that connects blocks i and j in the diagram) and $1 = \Theta_{ij} - (\Theta_{ij} - 1)$ (when no such line is present). In this way the total time factor of the contributing diagrams becomes a sum of terms of the form $[\Pi\Theta][\Pi(\Theta - 1)]$, which for the examples considered so far each give rise to a finite energy shift in the adiabatic limit. In this section we shall prove quite generally that the rearrangement procedure just described always leads to a sum of finite terms.

Each term in a rearranged time factor may be represented by a block diagram in which all lines between the blocks carry either a single or a double arrow, corresponding to functions Θ_{ij} and $\Theta_{ij} - 1$, respectively. Such a block diagram entails a divergent contribution in the energy shift if these functions permit a time ordering of the vertices in such a way that the time variables for the vertices of one or more blocks are all smaller than those of the rest of the diagram, so that these vertices may be isolated in time.

In principle, two types of divergent diagrams may show up: the blocks that can be isolated in the diagram will or will not be accompanied by parallel lines or even parallel strings of blocks (see fig. 8). Let us first treat the simple case without such a parallel structure. In fig. 8a a diagram of this type has been drawn. Both S_1 and S_2 stand for sets of blocks of which the internal structure (i.e. their constituent blocks and the single- or double-arrowed lines connecting them) need not be specified; only the lines that connect the sets of blocks have been displayed. A diagram of this general form will be divergent if the arrow configuration is such that the set S_1 and S_2 can be separated in time; in fact this is possible only if the arrows are drawn as in fig. 8a. The double arrow at the line l_2 stands for a factor $\Theta - 1$, which has emerged by writing $1 = \Theta - (\Theta - 1)$ in the original diagrams. Hence the latter have an intersection

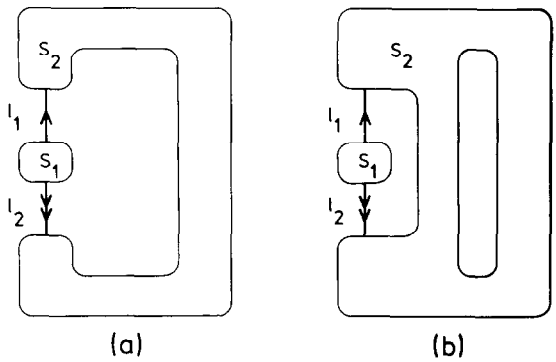

Fig. 8. Potentially divergent resummed diagrams, (a) without and (b) with parallel structure.

I through l_2 (*v.* fig. 9a). The single arrow at l_1 represents a factor Θ which has arisen either from a factor Θ or 1 in the underlying diagrams; so the intersection I' through l_1 may but need not be present there. Each original diagram without an intersection I' is thus associated with a similar diagram in which I' is realized. The number of intersections of these two diagrams differs by 1, so that they have an opposite sign (cf. (6)). As a consequence their contributions to the diagrams of fig. 8a exactly cancel. Thus a divergency of this form does not occur in the set of rearranged diagrams.

In the more general form of fig. 8b the set S_1 is accompanied by parallel lines or blocks belonging to S_2, so that the lines l_1 and l_2 do not represent the full initial or final state. A separation of S_1 and S_2 and hence a divergency is possible only if the lines l_1 and l_2 differ both in the type and the direction of their arrows. The example of fig. 8b is divergent as S_1 may be moved downward freely with respect to S_2.

Just as above we want to reconstruct the original block diagrams that lead

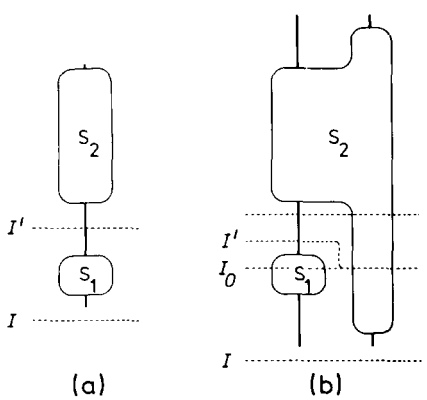

Fig. 9. Original diagrams underlying those of fig. 8, with their possible intersections.

in the rearrangement process to the diagram of fig. 8b. Again the line l_2, with double arrows, can result only from a factor $1 = \Theta - (\Theta - 1)$ and accordingly from an intersected line in the original block diagrams. Since l_2 represents only part of the initial state, this intersection I must also pass through S_2. The line l_1 corresponds to a factor Θ, which arises either from a factor Θ or $1 = \Theta - (\Theta - 1)$ in the original diagrams; consequently the latter diagrams have an intersection through l_2 and S_2 and possibly another intersection at l_1. One of these diagrams has been drawn in fig. 9b. Let I_0 be the highest intersection in this diagram that passes through S_2 and below l_1 (I_0 may be identical to I). The intersection I', which partially coincides with I_0 but in addition cuts through l_1, may be either present or absent. Hence such diagrams contribute to fig. 8b in pairs that differ only with respect to I'. Owing to the minus sign accompanying each intersection, however, the contributions of a pair cancel, as was found already for the special case of fig. 8a. Thus a diagram like fig. 8b does not occur either when the rearrangement of block diagrams is carried out. So we may conclude that the rearrangement procedure for the block diagrams leads indeed to a sum of terms that are separately convergent.

6. Block diagrams for the effective Hamiltonian

Up to now we have considered block-diagram representations for the averaged energy shift given by (6). We shall now show that such a representation can be used for the full effective Hamiltonian (5) as well. The main difference between the formulae (5) and (6) is the occurrence in the former of an additional product of θ functions, which specifies that the largest time variable is carried by one of the Hamilton operators in the first chronological product.

Let us once more consider the example of section 3, where the average energy shift has been evaluated for the two-photon exchange diagrams of fig. 1. For the full effective Hamiltonian the diagrams are evaluated analogously. In particular, the contributions with ground-level intermediate states from fig. 1a and 1c are again divergent. Their forms are similar to (10), with time factors F equal to:

$$\theta(t_{13})\theta(t_{24}) \tag{20}$$

for diagram 1a, and:

$$-\theta(t_{12})\theta(t_{13})\theta(t_{14}) - \theta(t_{21})\theta(t_{23})\theta(t_{24}) \tag{21}$$

for diagram 1c. The formula (21) expresses that in diagram 1c the largest time is associated with either vertex 1 or 2. As in section 3 the total time factor may be

rearranged such that the divergencies cancel:

$$\theta_{13}\theta_{24} - \theta_{12}\theta_{13}\theta_{14} - \theta_{21}\theta_{23}\theta_{24} = -\theta_{12}\theta_{13}\theta_{14}\theta_{42} - \theta_{21}\theta_{23}\theta_{24}\theta_{31}. \tag{22}$$

It may be verified that each of the terms at the right-hand side excludes an ordering of the vertices with a ground-level energy at intermediate times.

The above rearrangement procedure may again be formulated in terms of block diagrams. On a par with the diagrams of fig. 2 for the averaged energy shift the full effective Hamiltonian for the two-photon process is represented by the blocks of figs. 10a–c. In the present case the asterisk is necessary to label the blocks in which the vertex with the largest time variable is contained. (It should be noted that as a consequence of the simple internal structure of the blocks in this special case a diagram of the form of fig. 10d does not show up; for processes with a more complicated structure of the blocks this diagram will play a role as well.) Addition of the diagrams 10a and 10c leads to the diagram 10e in which the double arrow has the same meaning as before. From the figure a time factor:

$$(\Theta_{\mathrm{I,II}} - 1)[\theta(t_{12})\theta(t_{13})\theta(t_{14}) + \theta(t_{21})\theta(t_{23})\theta(t_{24})] \tag{23}$$

may be read off, which is indeed equivalent to (22). The finiteness of the rearranged diagram 10e is not guaranteed by closed loops of single or double arrows as in fig. 3, but by the fact that the asterisk in block I prevents block II to be moved to the top of the figure.

The general prescription for the rearrangement of the block diagrams into a sum of convergent contributions is the same as before: in the time factors of the factorized block diagrams a function $\Theta - (\Theta - 1)$ is introduced for each absent line between two blocks. The total time factor of a set of block diagrams with the same structure may be written then again as a product of functions Θ and $\Theta - 1$; in addition it also contains a factor that indicates the position of the vertex with the largest time variable.

Just as before a general proof can be given that the rearranged diagrams are separately convergent. The most general diagram to be considered has the structure of fig. 8b, with an asterisk in either S_1 or S_2. When the arrow configuration is as drawn in fig. 8b an asterisk in S_1 implies that the diagram

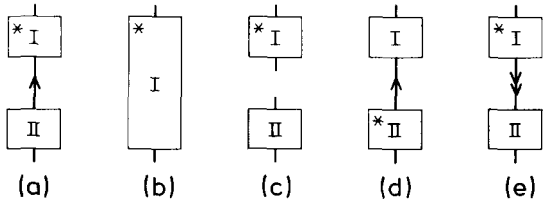

Fig. 10. Block diagrams for the effective Hamiltonian of the two-photon exchange process

remains finite, while for an asterisk in S_2 the argument of section 5 can be repeated. If the configuration with interchanged arrows is realized the asterisk must be chosen in S_2; in that case the contribution is again finite.

7. Connexion with the S matrix

In the preceding sections we have shown how the expansion in Feynman diagrams for the effective Hamiltonian (5) or (6) may be resummed such that the individual terms remain finite in the adiabatic limit. When in the expressions for V and Tr V the factors $\exp(-\epsilon|t|)$ are accordingly suppressed the functions $\delta(t_{\max})$ can be eliminated as well by employing time-translation invariance. To do so we first make the formal step of associating energies E_i and E_f with the initial and final projectors in (5) and (6). Upon shifting all time variables from t to $t+\tau$ these equations then remain invariant apart from the replacement:

$$\delta(t_{\max}) \to \delta(t_{\max}+\tau)\, e^{i(E_f-E_i)\tau}. \tag{24}$$

In the formulae thus obtained for V and Tr V we subsequently bring the exponential $\exp\{i(E_f-E_i)\tau\}$ to the left-hand side and integrate from $\tau=-\infty$ to $\tau=\infty$. As a result we get from (6) for instance:

$$\begin{aligned} &-2\pi\, i\delta(E_f-E_i)\,\mathrm{Tr}\, V \\ &= \sum_{n=1}^{\infty}(-i)^n \int_{-\infty}^{\infty} dt_1 \ldots dt_n \sum_{N=1}^{\infty} {\sum_{k_1,\ldots,k_N=1}^{\infty}}' \frac{(-1)^{N-1}}{N k_1! \ldots k_N!} \\ &\quad \times \mathrm{Tr}\{P_0 T[H_1(t_1)\ldots H_1(t_{k_1})] P_0 T[H_1(t_{k_1+1})\ldots H_1(t_{k_1+k_2})]\ldots \\ &\qquad P_0 T[H_1(t_{n-k_N+1})\ldots H_1(t_n)]\}. \end{aligned} \tag{25}$$

The equation (25) may be cast in a very suggestive form by relaxing the constraint on $\Sigma_{j=1}^{N} k_j$ through an interchange of the summations and time integrations, so that the sums over k_j become independent. Each of these reproduces the series expansion (2) for the operator $U(\infty,-\infty)-1$; thus we have:

$$-2\pi\, i\delta(E_f-E_i)\,\mathrm{Tr}\, V = \sum_{N=1}^{\infty} \frac{(-1)^{N-1}}{N} \mathrm{Tr}[P_0 U(\infty,-\infty) P_0 - P_0]^N, \tag{26}$$

which may be written as:

$$-2\pi\, i\delta(E_f-E_i)\,\mathrm{Tr}\, V = \mathrm{Tr}\log S \tag{27}$$

with $S = U(\infty,-\infty)$. So we have found from (6) a relation between the

averaged energy shift $\overline{\Delta E} = \mathrm{Tr}\, V/\mathrm{Tr}\, P_0$ and the S matrix[20]). It should be remarked that a straightforward evaluation of the S matrix by standard field-theoretical techniques will lead to divergencies in the result for Tr V; these divergencies are eliminated only when a resummation of the Feynman diagrams is performed in the way described in the preceding sections.

A result similar to (27) cannot be obtained from (5) for the operator V itself, owing to the additional θ functions in the integrand. However, the latter become superfluous if the sum $\Sigma_{N=1}^{\infty}$ occurring in (5) may be truncated after the first term; this is correct for instance if lowest-order perturbation theory is used. On a par with (27) we then get[11,19]):

$$-2\pi\, \mathrm{i}\delta(E_f - E_i)V = S - 1. \tag{28}$$

This relation may also be understood heuristically on the basis of the Born approximation[2]).

Appendix

The existence of the adiabatic limit in separate contributions to the effective Hamiltonian V has so far been judged directly from the structure of the corresponding Feynman diagrams. In fact, it was argued that a diagram yields a finite result if for each time ordering of the vertices the total energy $E(t)$ at an intermediate time t is always different from the initial or final energy $E_i = E_f = E(\pm\infty)$. This argument will now be considered in more detail.

After application of the Wick theorem to the equations (5) and (6) for V and Tr V the effective Hamiltonian is expressed in terms of propagators, which have the general form:

$$\langle 0|T[\phi(x_p)\bar{\phi}(x_q)]|0\rangle$$
$$= \theta(t_{pq}) \sum_{E>0} \phi(\boldsymbol{x}_p)\bar{\phi}(\boldsymbol{x}_q)\, \mathrm{e}^{-\mathrm{i}Et_{pq}} - \theta(t_{qp}) \sum_{E<0} \phi(\boldsymbol{x}_p)\bar{\phi}(\boldsymbol{x}_q)\, \mathrm{e}^{-\mathrm{i}Et_{pq}}, \tag{A.1}$$

for any of the fields $\phi(x)$ taking part in the interaction; the wave functions $\phi(\boldsymbol{x})$ belong to the single-particle eigenstates of the noninteracting system, with energy eigenvalues E. In the example of section 3 the fields $\phi(x)$ are the electromagnetic and Dirac-fields $A^{\mu}(x)$ and $\psi(x)$, respectively, of which the propagators are given in (8) and (9). In view of (A.1) the time integral $I^{(n)}$ of an nth-order contribution $V^{(n)}$ to V can be written as:

$$I^{(n)} = \lim_{\epsilon\to 0} \int \mathrm{d}t_1 \ldots \mathrm{d}t_n \delta(t_{\max}) \Big[\prod_{p=1}^{n} \mathrm{e}^{\mathrm{i}E_p t_p - \epsilon|t_p|}\Big] \prod \theta(t_{qr}). \tag{A.2}$$

The energies E_p are linear combinations of the eigenvalues E associated with

the propagators (pq), (qp) and the external initial and final lines (pi), (fp) that are connected to the vertex p. In fact one has:

$$E_p = \sum_f E_{fp} + \sum_q E_{qp} - \sum_q E_{pq} - \sum_i E_{pi}; \tag{A.3}$$

energy conservation then implies $\Sigma_{p=1}^{n} E_p = E_i - E_f = 0$.

We shall now derive the conditions under which $I^{(n)}$, and hence $V^{(n)}$, is finite in the adiabatic limit. To do so we may choose any specific time ordering of the vertices and replace the product $\Pi\theta(t_{qr})$ in (A.2) by a string of θ functions; let us take $t_1 > t_2 > \cdots > t_n$ and write:

$$\prod \theta(t_{qr}) = \prod_{q=2}^{n} \theta(t_{q-1,q}). \tag{A.4}$$

Substituting (A.4) in (A.2) and introducing the new integration variables $\tau_1 = -t_1$ and $\tau_p = t_{p-1} - t_p$, $p = 2, \ldots, n$, we get for the time integral:

$$\begin{aligned} I^{(n)} &= \lim_{\epsilon \to 0} \prod_{p=2}^{n} \int_{-\infty}^{\infty} d\tau_p \theta(\tau_p) \exp\left[i \left(\sum_{q=p}^{n} E_q \right) \tau_p - (n-p+1)\epsilon |\tau_p| \right] \\ &= \lim_{\epsilon \to 0} \prod_{p=2}^{n} \left[-i \left(\sum_{q=p}^{n} E_q \right) + (n-p+1)\epsilon \right]^{-1}. \end{aligned} \tag{A.5}$$

This result implies that the adiabatic limit exists if the sum $\Sigma_{q=p}^{n} E_q$ is different from zero for $p = 2, \ldots, n$. With (A.3) the latter becomes:

$$\sum_{q=p}^{n} E_q = \sum_{f,q(q \geqq p)} E_{fq} + \sum_{q,r(q \geqq p > r)} E_{rq} - \sum_{q,r(q \geqq p > r)} E_{qr} + \sum_{i,q(q<p)} E_{qi}. \tag{A.6}$$

The right-hand side may be written as the difference between the intermediate energy $E(t)$, for $t_{p-1} > t > t_p$, and the initial energy $E_i = E(-\infty)$. The former is associated with an intersection of the diagram at a fixed time t and is defined as:

$$E(t) = \sum_{f,p(t>t_p)} E_{fp} + \sum_{p,q(t_p>t>t_q)} E_{pq} - \sum_{p,q(t_p>t>t_q)} E_{qp} + \sum_{p,i(t_p>t)} E_{pi}, \tag{A.7}$$

independent of the specific choice (A.4). So we conclude that the adiabatic limit exists if $E(t)$ always differs from the initial energy $E(-\infty)$. From (A.5) it is clear that in this case the limit may already be carried out inside the time integral, provided that the Fourier transform of the θ function is taken to be:

$$\int_{-\infty}^{\infty} d\tau \theta(\tau) e^{-iE\tau} = \frac{-i}{E - i0}, \tag{A.8}$$

which is the form generally used in the Feynman formalism.

Acknowledgements

This investigation is part of the research programme of the "Stichting voor Fundamenteel Onderzoek der Materie (FOM)", which is financially supported by the "Nederlandse Organisatie voor Zuiver-Wetenschappelijk Onderzoek (Z.W.O.)".

References

1) P.J. Ellis and E. Osnes, Rev. Mod. Phys. **49** (1977) 777.
R. Lefebvre and C. Moser, eds., Correlation effects in Atoms and Molecules, Advances in Chemical Physics **14** (Wiley, New York, 1969).
2) A.I. Akhiezer and V.B. Berestetskii, Quantum Electrodynamics (Moscow, 1953) (in Russian; English translation Interscience, New York, 1965).
3) T. Morita, Progr. Theor. Phys. **29** (1963) 351.
4) G. Oberlechner, F. Owono-N'-Guema and J. Richert, Nuovo Cimento **68B** (1970) 23.
5) T.T.S. Kuo, S.Y. Lee and K.F. Ratcliff, Nucl. Phys. **A176** (1971) 65.
6) I.E. Dzialoshinskii, Sov. Phys. JETP **3** (1956) 977.
7) C. Mavroyannis and M.J. Stephen, Mol. Phys. **5** (1962) 629.
8) L.N. Labzovskii, Sov. Phys. JETP **32** (1971) 94.
9) M.A.J. Michels and L.G. Suttorp, Physica **67** (1973) 137.
10) M.A.J. Michels and L.G. Suttorp, Mol. Phys. **33** (1977) 245.
11) M.A.J. Michels, The long-range interaction of relativistic hydrogen atoms, thesis, University of Amsterdam (1976).
12) L.G. Suttorp and M.A.J. Michels, Chem. Phys. Lett. **46** (1977) 391.
13) C. Bloch, Nucl. Phys. **6** (1958) 329.
14) D.J. Klein, J. Chem. Phys. **61** (1974) 786.
15) M. Gell-Mann and F. Low, Phys. Rev. **84** (1951) 350.
16) L.N. Bulaevskii, Sov. Phys. JETP **24** (1967) 154.
17) Y. Dmitriev, Int. J. Quant. Chem. **9** (1975) 1033.
18) V.V. Tolmachev, Adv. Chem. Phys. **14** (1969) 421.
19) M.A.J. Michels and L.G. Suttorp, Physica **93A** (1978) 559.
20) M.A.J. Michels and L.G. Suttorp, J. Phys. A (to be published).
For the nondegenerate case see J. Hubbard, Proc. Roy. Soc. **A240** (1957) 539; L.S. Rodberg, Phys. Rev. **110** (1958) 277; P. Nozières, Theory of Interacting Fermi Systems (Benjamin, New York, 1964); ref. 19.